Magnetic Nanoparticles

DOI: 10.1002/ange.201005600

From Hot-Injection Synthesis to Heating-Up Synthesis of Cobalt Nanoparticles: Observation of Kinetically Controllable Nucleation**

Jaakko V. I. Timonen, Eira T. Seppälä, Olli Ikkala, and Robin H. A. Ras**

Monodisperse nanoparticles of well-defined size and shape are required in several emerging applications, which take advantage of their size-dependent properties such as the superparamagnetic limit in the case of magnetic nanoparticles.[1,2] Accurate tuning of the nanoparticle size and shape requires understanding of the mechanisms involved in particle nucleation and growth.[3–5] In spite of extensive ongoing research, these mechanisms are still not fully understood owing to their complexity and interplay. Moreover, the current small-scale synthesis methods, such as the hot-injection method, can be difficult to scale to industrially relevant levels. Hence, more suitable methods are sought.[6–19]

Herein, we revisit a widely studied hot-injection synthesis of monodisperse cobalt nanoparticles[20–26] and show that the particle nucleation differs from what is expected for a hot-injection synthesis. Evidence is given that the particles nucleate several tens of seconds or a few minutes after the injection, depending delicately on how the reaction temperature is controlled after the sudden temperature drop caused by the injection. The delayed nucleation is followed by a period during which the cobalt precursor decomposes endothermically, the temperature drops, carbon monoxide evolves, and the nuclei rapidly grow into mature nanoparticles. Particle growth after the endothermic period is negligible, and we show that the final particle size is determined by the rate of temperature increase after the injection-induced temperature drop. A rapid increase results in a higher peak temperature before the endothermic period and more nuclei, hence smaller particles, in comparison to the case of a slower rate of temperature increase. The contribution of the injection to particle nucleation seems minor, and it is shown that injection can be replaced entirely by an accurately controlled heating up of the solution containing all reagents (including the cobalt precursor) from room temperature to the nucleation temperature. This synthetic method, which is often termed either "non-injection synthesis"[15,16] or "heating-up synthesis",[3,11] results in nanoparticles that are nearly identical to those made by the hot-injection method.

We synthesized cobalt nanoparticles by injecting dicobalt octacarbonyl, $[Co_2(CO)_8]$, dissolved in a small amount of *ortho*-dichlorobenzene (*o*-DCB, b.p. 181 °C) into a solution of oleic acid and trioctylphosphine oxide (TOPO) in *o*-DCB at reflux.[20] The injection led to an immediate temperature drop of several tens of degrees, which is characteristic of the hot-injection method in general.[4] It has been shown that $[Co_2(CO)_8]$ undergoes partial decarbonylation during the injection to form gaseous carbon monoxide and intermediate cobalt carbonyl species (e.g. tetracobalt dodecacarbonyl, $[Co_4(CO)_{12}]$, and cobalt tetracarbonyl, $[Co(CO)_4]$) in the solution phase; these species then further decompose more slowly to cobalt atoms.[25,27] It has been shown that both maintaining the lower temperature and letting the temperature recover to the reflux temperature after the injection can lead to monodisperse nanoparticles.[20–23] In this study, we concentrated on the latter approach and studied for the first time in detail the kinetics of the temperature recovery to reflux. The recovery rate can be conveniently controlled by tuning the rate of heat transfer from the heat bath to the reaction medium, for example, by using an oil bath at different temperatures or an electric heating mantle with different heating powers.

A typical development in the reaction temperature after the injection is shown in Figure 1 for the hot-injection synthesis HI1 (see the Experimental Section for a complete list of syntheses with details). The temperature dropped from 180 to 143 °C during the injection, after which it started to recover, as heat was being transferred from the heat bath to the reaction medium. In contrast to the expected continuous increase until the reflux temperature was reached, one minute after the injection we observed a characteristic endothermic period during which the reaction temperature dropped despite continuous heating. Interestingly, the peak temperature (174 °C) reached just before the endothermic period was very close to the temperature prior to injection (180 °C). Vigorous evolution of carbon monoxide during the endothermic period indicated decomposition of the cobalt carbonyl species and release of cobalt atoms.[27] Further evolution of carbon monoxide after the endothermic period was negligible, even when the reflux temperature was reached. This observation indicated that nearly all cobalt carbonyl species had decomposed during the endothermic period, which was

[*] J. V. I. Timonen, Prof. Dr. O. Ikkala, Dr. R. H. A. Ras
Department of Applied Physics, Aalto University
(formerly Helsinki University of Technology)
P.O. Box 15100, FI-02150 Espoo (Finland)
E-mail: jaakko.timonen@tkk.fi
robin.ras@tkk.fi
Homepage: http://tfy.tkk.fi/molmat/
Dr. E. T. Seppälä
Nokia Research Center
Itämerenkatu 11–13, 00180 Helsinki (Finland)

[**] Funding from Nokia Research Center, the Finnish Funding Agency for Technology and Innovation (Tekes), and the Academy of Finland is acknowledged. Electron microscopy images were obtained at the Nanomicroscopy Center at Aalto University. Dr. Christoffer Johans (Aalto University), Dr. Markku Oksanen (Nokia Research Center), and Dr. Andreas Walther (Aalto University) are acknowledged for fruitful discussions.

Supporting information for this article is available on the WWW under http://dx.doi.org/10.1002/anie.201005600.

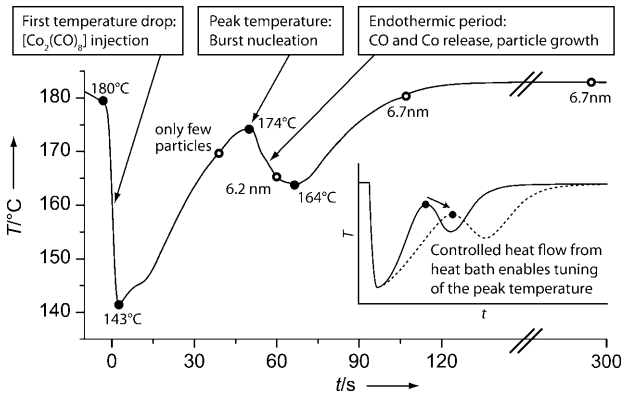

Figure 1. Typical double-drop of the reaction temperature in the hot-injection synthesis HI1: the second temperature drop is an endothermic period between 50 and 65 s. Temperature readings are marked as filled circles and particle diameters as observed by TEM as open circles (see the Supporting Information for TEM images and particle-size distributions).

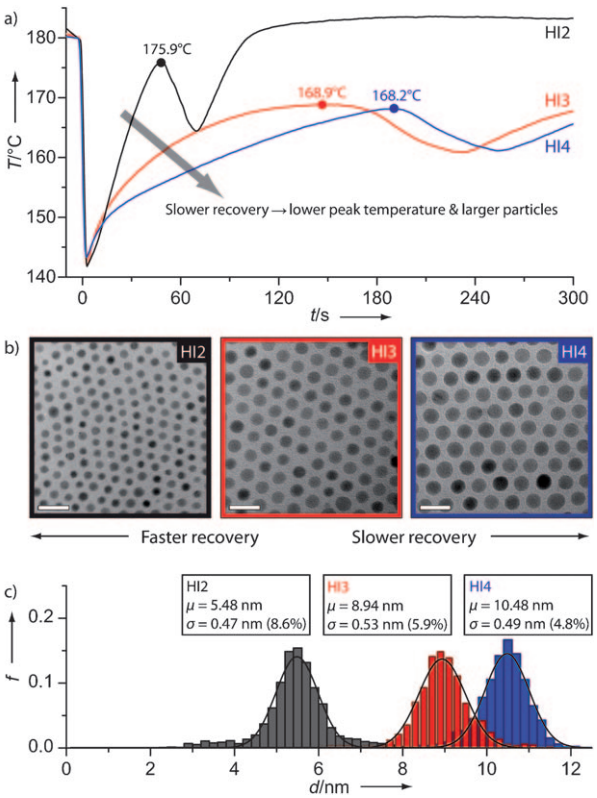

Figure 2. Effect of the temperature-recovery rate on the size distribution of the nanoparticles. a) Temperature histories. HI2: rapid temperature recovery, HI3: medium-rate recovery, HI4: slow recovery. b) Corresponding TEM images of full-grown particles (scale bars are 20 nm). c) Corresponding particle size distributions with Gaussian fits.

verified also by Fourier transform infrared spectroscopy (FTIR). Small aliquots were extracted during the synthesis and cast immediately on carbon-coated transmission electron microscopy (TEM) grids. TEM analysis indicated that very few nanoparticles existed in the reaction medium before the peak temperature, whereas after that point the medium was concentrated with nanoparticles. Determination of the average particle diameter as a function of reaction time and temperature indicated that the main growth took place during the endothermic period, and that growth thereafter was negligible (Figure 1). This result is in agreement with the observed decomposition of the precursor during the endothermic period. After that period, the particles were considered to be full-grown; further annealing at 180 °C or storage at room temperature resulted in negligible increase in particle size (see the Supporting Information).

The effect of the temperature-recovery rate on the peak temperature and on the resulting nanoparticles was investigated in syntheses HI2–HI4. These syntheses were similar to HI1, except that the temperature-recovery rate after the injection was varied by tuning heat transfer to the reaction medium (HI2: rapid temperature recovery owing to a high temperature of 215 °C of the heating oil bath, HI3: medium-rate recovery owing to a lower temperature of 195 °C of the heating oil bath, HI4: slow recovery owing to the very low heating power of an electric heating mantle). The temperature histories of these syntheses (Figure 2a) featured qualitatively similar double-drop behavior as observed in HI1. However, a decrease in the heating rate led to a decrease in the peak temperature reached before the endothermic period and also to a decrease in the magnitude of the temperature drop. Furthermore, the endothermic period shifted toward later times as the recovery rate decreased. Despite these differences, the growth pattern of the nanoparticles was qualitatively the same as in HI1. That is, the particles appeared very close to the peak temperature, and the main growth took place during the endothermic period. Importantly, the average diameter of the full-grown particles from HI2–HI4 was also dependent on the recovery rate. The trend of an increasing particle size with a decreasing temperature-recovery rate is clear from the TEM images of the full-grown nanoparticles (Figure 2b) and the corresponding particle size distributions (Figure 2c).

It has been suggested that nucleation in the studied synthesis takes place nearly instantaneously during the injection.[21] Our results from syntheses HI1–HI4 suggest another mechanism. The nearly complete absence of particles before the peak temperature and the rapid appearance of particles after the peak temperature already suggest that the nucleation takes place near the peak temperature instead of the injection. Unfortunately, although the direct measurement of nuclei concentration and size distribution is well-established for optically active quantum-dot nanoparticles, it is more difficult for particles that are not optically active, such as cobalt nanoparticles.[11,28–31] Therefore, we used an indirect method to resolve the final concentration of the full-grown nanoparticles. The concentration can be calculated from the amount of carbonyl present initially and the average size of the nanoparticles at the end of the synthesis if the conversion of cobalt into nanoparticles (crystallization yield) is known. We determined the crystallization yield to be approximately 90 % in these syntheses (see the Supporting Information); hence, the concentrations of the full-grown nanoparticles and also the nuclei are approximately 24.9 μM (HI2), 5.7 μM (HI3),

and 3.6 μM (HI4). This variation in the concentration cannot be explained by random variation in the number of nuclei formed during the injection since special care was taken to make the injections identical: the injection was always started at 180.0 ± 0.5 °C, its duration was intentionally stretched to 5 s, and the lowest temperature reached was always observed to be 143.0 ± 1.0 °C. No difference in the final particles was observed if the injection was carried out more rapidly (in less than 1 s). Moreover, the temperature behavior during the first 15 s after the injection was almost the same in all syntheses as a result of dominant heat transfer from the reaction-vessel walls rather than from the heat bath (Figure 2a). Hence, the difference in the final particle size stems from reactions taking place after the first 15 s and before the end of the endothermic period (after which growth is terminated).

In some hot-injection syntheses of other nanoparticles, the number of nuclei formed during the injection is initially high, but afterwards some nuclei dissolve back to monomers. Thus, the nuclei concentration is decreased, and the remaining nuclei can grow into larger particles.[28–30] However, the partial dissolution of nuclei is not the reason for the formation of differently sized nanoparticles at different temperature-recovery rates in the synthesis under investigation: the hot-injection synthesis HI2 was successfully converted into a heating-up synthesis HU1, in which the injection of the carbonyl compound was replaced by mixing of the carbonyl compound directly with all the other reagents at room temperature and heating of the solution to reflux. The heating rate was adjusted to be very close to that of HI2 near the peak temperature, and a very similar temperature drop resulted (Figure 3a). Furthermore, the particles formed in the heating-up synthesis appeared similarly in the vicinity of the peak temperature and had approximately the same size of 5 nm as in the hot-injection synthesis (Figure 3b). This similarity between the hot-injection and heating-up methods indicates that the injection has only a minor effect on nucleation, since it can be omitted without a notable change in the nanoparticles. If there was nucleation during the injection, practically all nuclei would redissolve after the injection and reform after a delay just before the endothermic period. The particles synthesized by the heating-up method were characterized by high-resolution TEM, electron diffraction, and magnetometry (see the Supporting Information), which indicated that the particles were superparamagnetic and single-crystalline ε-cobalt, like those formed by the hot-injection synthesis.

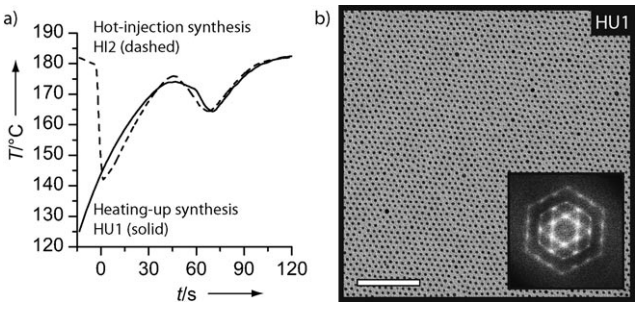

Figure 3. Comparison of the hot-injection and heating-up methods. a) Temperature histories of the HI2 and HU1 syntheses under identical conditions (same reagents and heating rate). b) TEM image of full-grown particles from HU1 (scale bar is 100 nm; inset shows diffractogram of the image).

To demonstrate that nucleation in the heating-up synthesis can be controlled by temperature kinetics as in the hot-injection method, we performed two heating-up syntheses with different heating rates. In HU2, the flask containing the precursor reagents was heated rapidly by immersing it in an oil bath at 215 °C, whereas in HU3, the heating rate was slower as a result of a lower temperature of 195 °C of the oil bath (Figure 4a). Both syntheses exhibited a temperature peak near 170 °C, which was followed by an endothermic period. The diameters of the full-grown nanoparticles showed a standard deviation of only 7% in both cases. However, the particles produced during more rapid heating were considerably smaller than those produced during slower heating (Figure 4b). Because of the similar crystallization yield in both cases, more nuclei had to form under the conditions of more rapid heating.

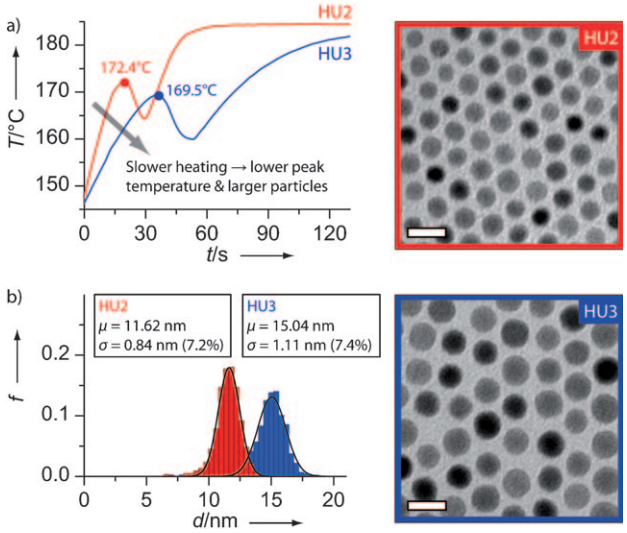

Figure 4. Temperature control of nanoparticle size in the heating-up synthesis. a) Temperature histories of HU2 (rapid heating) and HU3 (slow heating). b) Corresponding particle size distributions with Gaussian fits. Corresponding TEM images of full-grown particles are shown on the right. Scale bars are 20 nm.

The experimental observations can be discussed in terms of nucleation theory to shed more light on the formation of the nanoparticles, even though the exact chemical composition of the particle-forming monomer often cannot be resolved.[5,11] Nucleation becomes thermodynamically increasingly favorable as the concentration of the monomers increases beyond the saturation limit.[3,4] In an ideal hot-injection synthesis, the monomer concentration greatly exceeds the saturation limit during the injection, which results in very rapid burst nucleation. Our observations suggest that during injection in the studied synthesis, the saturation limit is not exceeded enough for burst nucleation to happen. Instead, the experimental results can be understood if the injection

only causes a preliminary increase in the monomer concentration, which continues to increase after the injection as the carbonyl species decompose (which is observed as slow evolution of carbon monoxide before the peak temperature and which has also been shown by in situ Fourier transform infrared spectroscopy (FTIR)[25]). When the monomer concentration reaches the burst-nucleation limit, the particles nucleate and grow rapidly (as demonstrated in Figure 1) along with more intensive evolution of carbon monoxide (as also observed by FTIR[25]). Similar delayed nucleation after precursor injection has been observed in the synthesis of iron oxide nanodisks,[32] and a similar gradual increase in monomer concentration during the heating up of iron oleate has been shown to lead to the nucleation of monodisperse iron oxide nanoparticles.[11]

Both the peak temperature around which nucleation takes place and the number of nuclei formed increase with the heating rate. This correlation may be understood by considering the rate of monomer formation. Since the decomposition of cobalt carbonyl complexes is more rapid at higher temperatures,[27] the burst-nucleation limit is reached in less time under conditions of rapid heating (HI2 and HU2), and hence the temperature at the nucleation point is higher than under conditions of slower heating (HI3,4 and HU3). A higher temperature during the nucleation results in more rapid monomer formation, which partially compensates for the monomers consumed in the nucleation and thus enables more nuclei to be formed before growth takes over. Another contribution to the increased number of nuclei comes from the nucleation process itself, which is more rapid at higher temperatures.[5] The temperature drop due to the endothermicity of the decomposition of cobalt carbonyl complexes can also play a role in particle formation, since a decrease in temperature can help quench the nucleation.

Significant effort has been made recently in the development of techniques for the large-scale synthesis of monodisperse nanoparticles, such as different heating-up[6,9–19] and pressure-drop methods.[7,8] One advantage of the presented heating-up synthesis is that it can be readily scaled to multigram quantities (see the Supporting Information for a one-pot heating-up synthesis with a yield of about 2 g of particles). Furthermore, the heating-up synthesis may enable the development of an industrially relevant continuous-flow process in which the temperature of the precursor solution is increased in a controlled way to the nucleation temperature while the evolving carbon monoxide is removed from the system.

Even though the hot-injection synthesis of cobalt nanoparticles has been investigated intensively, no detailed information on the temperature development and its effect on the nanoparticles have been provided previously. Kinetic control of the nucleation may explain why differently sized particles have been obtained under otherwise identical conditions (same injection temperature and reagents).[20–23,33] The kinetics of carbon monoxide formation and removal are also relevant, but have been studied less.[7,8] They may play some role, as carbon monoxide controls metal-nanostructure growth.[34] We also demonstrated that other types of cobalt carbonyl complexes, such as $[Co_4(CO)_{12}]$, can be used in the heating-up synthesis to produce nanoparticles (see the Supporting Information). Finally, even though the injection was shown to be less important than previously suggested, at least in the case where the temperature is raised back to reflux after the injection, the injection may still have significance since precursor decomposition and complexation with surfactants may proceed differently in the heating-up synthesis compared to the hot-injection synthesis. Such a difference may explain why the heating-up method results in somewhat broader polydispersity than the hot-injection method.

In conclusion, it has been shown that the number of nuclei formed in the hot-injection synthesis of cobalt nanoparticles depends more on temperature kinetics after the injection than on the injection itself. We suggest that the injection leads to supersaturation that is not high enough to cause burst nucleation, and hence the nucleation is delayed until enough monomers are created from the decomposing precursor. The number of nuclei formed in the delayed nucleation can be controlled by kinetic tuning of the temperature at which the nucleation takes place. This insight led to a technologically relevant heating-up synthesis of nearly monodisperse cobalt nanoparticles that is readily scalable to a multigram level and in which the particle size can be controlled simply by the heating rate.

Experimental Section

Hot-injection syntheses HI1–HI4: $[Co_2(CO)_8]$ (1080 mg) dissolved in *o*-DCB (6 mL) was injected into a solution of TOPO (200 mg) and oleic acid (360 mg, 0.4 mL) in *o*-DCB (24 mL) at 180 ± 0.5 °C under N_2. Postinjection temperature recovery was tuned by adjusting heat transfer from the heat bath to the reaction medium to either rapid (HI1 and HI2: an oil bath with efficient heat transfer and a high set temperature of 215 °C), medium (HI3: as HI1 and HI2, but with a lower set temperature of 195 °C), or slow (HI4: electric heating mantle with reduced heat transfer).

Heating-up synthesis HU1: As for HI1 and HI2, except that all reagents were mixed at room temperature, followed by heating to reflux by immersion of the flask in the oil bath. Heating-up syntheses HU2 and HU3: A solution of $[Co_2(CO)_8]$ (1080 mg), TOPO (300 mg), and oleic acid (270 mg, 0.3 mL) in *o*-DCB (30 mL) was heated under N_2 to reflux either rapidly (HU2: by immersion of the flask in an oil bath at 215 °C) or slowly (HU3: by immersion of the flask in an oil bath at 195 °C).

See the Supporting Information for synthesis details.

Received: September 7, 2010
Revised: December 7, 2010
Published online: January 26, 2011

Keywords: cobalt · hot-injection method · nanoparticles · nucleation · synthetic methods

[1] Z. Nie, A. Petukhova, E. Kumacheva, *Nature Nanotech.* **2010**, *5*, 15.
[2] V. Skumryev, S. Stoyanov, Y. Zhang, G. Hadjipanayis, D. Givord, J. Nogues, *Nature* **2003**, *423*, 850.
[3] J. Park, J. Joo, S. G. Kwon, Y. Jang, T. Hyeon, *Angew. Chem.* **2007**, *119*, 4714; *Angew. Chem. Int. Ed.* **2007**, *46*, 4630.
[4] C. de Mello Donegá, P. Liljeroth, D. Vanmaekelbergh, *Small* **2005**, *1*, 1152.

[5] E. V. Shevchenko, D. V. Talapin, H. Schnablegger, A. Kornowski, Ö. Festin, P. Svedlindh, M. Haase, H. Weller, *J. Am. Chem. Soc.* **2003**, *125*, 9090.
[6] N. A. D. Burke, H. D. H. Stöver, F. P. Dawson, *Chem. Mater.* **2002**, *14*, 4752.
[7] C. Johans, M. Pohjakallio, M. Ijäs, Y. Ge, K. Kontturi, *Colloids Surf. A* **2008**, *330*, 14.
[8] M. Huuppola, N. Doan, K. Kontturi, C. Johans, *J. Colloid Interface Sci.* **2010**, *344*, 292.
[9] M. M. Bull, W. J. Chung, S. R. Anderson, S.-j. Kim, I.-B. Shim, H.-j. Paik, J. Pyun, *J. Mater. Chem.* **2010**, *20*, 6023.
[10] J. Park, K. An, Y. Hwang, J.-G. Park, H.-J. Noh, J.-Y. Kim, J.-H. Park, N.-M. Hwang, T. Hyeon, *Nature Mater.* **2004**, *3*, 891.
[11] S. G. Kwon, Y. Piao, J. Park, S. Angappane, Y. Jo, N.-M. Hwang, J.-G. Park, T. Hyeon, *J. Am. Chem. Soc.* **2007**, *129*, 12571.
[12] Y. C. Cao, J. Wang, *J. Am. Chem. Soc.* **2004**, *126*, 14336.
[13] Y. A. Yang, H. Wu, K. R. Williams, Y. C. Cao, *Angew. Chem.* **2005**, *117*, 6870; *Angew. Chem. Int. Ed.* **2005**, *44*, 6712.
[14] L. Li, P. Reiss, *J. Am. Chem. Soc.* **2008**, *130*, 11588.
[15] T.-Y. Liu, M. Li, J. Ouyang, M. B. Zaman, R. Wang, X. Wu, C.-S. Yeh, Q. Lin, B. Yang, K. Yu, *J. Phys. Chem. C* **2009**, *113*, 2301.
[16] J. Ouyang, J. Kuijper, S. Brot, D. Kingston, X. Wu, D. M. Leek, M. Z. Hu, J. A. Ripmeester, K. Yu, *J. Phys. Chem. C* **2009**, *113*, 7579.
[17] L. M. Bronstein, X. Huang, J. Retrum, A. Schmucker, M. Pink, B. D. Stein, B. Dragnea, *Chem. Mater.* **2007**, *19*, 3624.
[18] A. Puglisi, S. Mondini, S. Cenedese, A. M. Ferretti, N. Santo, A. Ponti, *Chem. Mater.* **2010**, *22*, 2804.
[19] Y. Chen, E. Johnson, X. Peng, *J. Am. Chem. Soc.* **2007**, *129*, 10937.
[20] V. F. Puntes, K. M. Krishnan, A. P. Alivisatos, *Science* **2001**, *291*, 2115.
[21] V. F. Puntes, D. Zanchet, C. K. Erdonmez, A. P. Alivisatos, *J. Am. Chem. Soc.* **2002**, *124*, 12874.
[22] A. C. S. Samia, K. Hyzer, J. A. Schlueter, C.-J. Qin, J. S. Jiang, S. D. Bader, X.-M. Lin, *J. Am. Chem. Soc.* **2005**, *127*, 4126.
[23] Y. Bao, W. An, C. H. Turner, K. M. Krishnan, *Langmuir* **2010**, *26*, 478.
[24] G. Cheng, C. L. Dennis, R. D. Shull, A. R. H. Walker, *Langmuir* **2007**, *23*, 11740.
[25] A. Lagunas, C. Jimeno, D. Font, L. Solà, M. A. Pericàs, *Langmuir* **2006**, *22*, 3823.
[26] G. Cheng, J. D. Carter, T. Guo, *Chem. Phys. Lett.* **2004**, *400*, 122.
[27] R. Tannenbaum, G. Bor, *J. Organomet. Chem.* **1999**, *586*, 18.
[28] C. R. Bullen, P. Mulvaney, *Nano Lett.* **2004**, *4*, 2303.
[29] J. van Embden, P. Mulvaney, *Langmuir* **2005**, *21*, 10226.
[30] M. Tiemann, Ö. Weiß, J. Hartikainen, F. Marlow, M. Lindén, *ChemPhysChem* **2005**, *6*, 2113.
[31] B. Abécassis, F. Testard, O. Spalla, P. Barboux, *Nano Lett.* **2007**, *7*, 1723.
[32] M. F. Casula, Y.-w. Jun, D. J. Zaziski, E. M. Chan, A. Corrias, A. P. Alivisatos, *J. Am. Chem. Soc.* **2006**, *128*, 1675.
[33] G. Cheng, D. Romero, G. T. Fraser, A. R. Hight Walker, *Langmuir* **2005**, *21*, 12055.
[34] Y. Kang, X. Ye, C. Murray, *Angew. Chem.* **2010**, *122*, 6292; *Angew. Chem. Int. Ed.* **2010**, *49*, 6156.

